Investigation of Flow Parameters and Efficiency of Mixture Separation on a Structured Packing

Aleksandr Pavlenko, Vladimir Zhukov, Nikolay Pecherkin, Vladimir Chekhovich, and Oleg Volodin
Kutateladze Institute of Thermophysics SB RAS, Novosibirsk 630090, Russia

Alexey Shilkin and Christoph Grossmann
BASF SE, Ludwigshafen D-67056, Germany

DOI 10.1002/aic.14298
Published online December 5, 2013 in Wiley Online Library (wileyonlinelibrary.com)

Results of experimental study of the effect of initial maldistribution of structured packing irrigation on efficiency of binary mixture separation are presented in this article. The studies were carried out in the experimental distillation column with the diameter of 0.9 m *using the R114 and R21 freon mixture. Experiments were performed on the structured Mellapak 350.Y packing of stainless steel 316L, containing 19 layers with the total height of 4.016* m *at the ratio of mole liquid and vapor flow rates L/V = 1 and 1.7, respectively, and the pressure in the upper part of the column* $p_{top} = 3$ bars. *Nonuniformity at the packing inlet was generated via the blocking of some holes in the liquid distributor. Here, we present some results on efficiency of mixture separation, pressure drop on the packing, distribution of local liquid flow rate under the packing over the cross-section and on the column wall within the range of vapor loading factor* ($0.69 < F_v < 1.61$ $Pa^{0.5}$), *as well as experimental data on distribution of local concentration of the low-boiling component over the cross-section and along the height of the structured packing. It is found out that significant maldistribution of mixture concentration and liquid flow rate over the cross-section slightly changes along the height in the lower part of the column at a change in the degree of packing irrigation nonuniformity at the inlet. It is shown that efficiency of mixture separation depends considerably on the value of parameter L/V, vapor flow factor* F_v, *and size of the zone underirrigated by liquid at the inlet. In the studied range of liquid and vapor flow rates, the relative pressure drop on the packing does not depend on the ratio of liquid and vapor flow rates L/V and degree of irrigation maldistribution.*
 AIChE J, 60: 690–705, 2014
Keywords: distillation column, structured packing, maldistribution, nonuniform liquid irrigation, efficiency of mixture separation

Introduction

Distillation is the most important process used in practice at separation of mixtures, and separation efficiency is one of the main parameters that determine the operating costs, capital costs, and equipment dimensions. The experimental and operating results of industrial distillation columns with regular packing show that separation efficiency often decreases with an increase in their diameter, and this affects the performance and purity of finished products. Basic phenomena responsible for a decrease in separation efficiency are the effects caused by transverse maldistribution and longitudinal mixing. These effects relate to the vapor and liquid flows inside the column and are characterized by deviation of column productivity and purity of the product against the design values for ideal conditions of uniform distribution. The published results of experiments carried out at the laboratory setups with the small packing diameter of columns demonstrate the efficiency of about 20 or more theoretical stages of separation per 1 m of the packing height, whereas the efficiency of the best industrial rigs is 5–6 theoretical stages per 1 m of the height.[1] Intensive research on the liquid and vapor flows dynamics, separation processes, and description of the separation efficiency calculation methods in the packing columns of different types are underway.[2–4] The relevant techniques for comparing the experimental data using the parameters determining separation efficiency on the structured packing in the columns of different diameters for different mixtures are discussed in Olujic[5] based on detailed analysis of publications. The goal of Olujic's[5] research was collection and evaluation of relevant publicly available information, and coming with a proposal for standardization of structured packing efficiency measurements, which, in turn, should lead toward obtaining of more reliable basic performance data to be used with more confidence in (re)design of industrial packed columns.

There are many reasons causing development of nonuniform liquid and vapor flows within the structured packing depending on the nature of their origin. The reasons which attract the most attention are associated with the design and manufacture of devices used for liquid and vapor distribution at the packing inlet.[6] The important role in mixture

Correspondence concerning this article should be addressed to A. Pavlenko at pavl@itp.nsc.ru.

separation efficiency is played by liquid redistribution, development of unwetted zones, or zones with a stagnant liquid film on the surface of corrugated sheets of the structured packing, studied, for instance, in papers.[7,8] The influence of liquid accumulation on the vertical edges of the structured packing near the column wall as a result of its redistribution over the sheets' surface on the efficiency of mixture separation is studied theoretically by Trifonov et al.[9] However, there is a mechanism, which is not usually considered and which relates to the fact that the vapor density in the upper part of distillation columns can be significantly higher than that in the lower part. The estimates show that sometimes an increase in the density of vapor flowing upward in the column due to a change in concentration and temperature more than by an order or two exceeds the reverse change in vapor density caused by a decrease in pressure along the height of the structured packing. As a result, the significant difference in the vapor density caused by the difference in concentration and temperature of the mixture along the packing height at low vapor velocities leads to the loss of stability under the conditions of the so-called negative stratification. Here, we have in mind that for some systems at mixture separation the vapor density increases significantly with its upward flow along the packing. This can lead to formation of significant large-scale nonuniformity of the local flow parameters in the packing cross-section as it is shown by Pavlenko et al.[10] The character of liquid and vapor flow nonuniformity development over the column cross-section and height is mainly determined by geometric characteristics of the packing. The methods of mathematical modeling of liquid flow over the elements of structured packing, allowing implementation of different types of nonuniformity and their effect on separation efficiency, become widespread in recent years.[9,11–15] Research on the complex catalytic systems with the use of structured packing is in progress as well.[16,17]

However, thorough consideration of the above factors combined with modeling of mixture separation processes on the structured packing is a very complex problem which to date has not been solved. At the same time, the exact knowledge about separation efficiency and the ability to compare it reasonably for the different types of the packing in the columns of different diameters with different parameters of internal units and devices (e.g., liquid and vapor distributors and redistributors, supporting grids etc.) is an issue of central importance for the chemical industry. As noted by Ottenbacher et al.,[18] today the experimental data are the only source of reliable information in this field of industry.

The importance of setting the optimum initial liquid distribution for dumped and structured packing is noted by Perry et al.[19] and Bonilla.[20] The liquid distributors with outflow through the holes are the complex and expensive parts of distillation columns, designed to provide uniform initial distribution of liquid. The drip point density and the pattern of drip point location relative to the packing elements are their basic parameters. The drip point density can vary from 10 to 1000 m^{-2}, whereas the drip point pattern can be triangular, rectangular, and square. The arrangement configuration of drip points is chosen for each type of the packing to ensure the irrigation of maximal number of packing elements with minimal flow nonuniformity. As the number of drip points can not be infinite, a part of the packing surface of the first layers remain always dry, that can lead to a decrease in separation efficiency because of a decrease in the mass-transfer surface. At long-term column operation, some distributor holes can be clogged partially or completely, and then the effect of the initial maldistribution can increase multifold. In some cases, liquid nonuniformity at the packing inlet can be caused by installation of various structures inside the column, such as liquid redistributors, supporting grids and so forth. As liquid flows over the packing and interacts with the vapor phase, nonuniformity can be developed due to the geometrical characteristics of the packing. Liquid distribution becomes significantly nonuniform in the near-wall and central parts of the column cross-section, moreover, some portion of liquid flows to the column wall. In this connection, wettability of the packing material is very important. To reduce the effect of liquid maldistribution on separation efficiency in the high columns it is recommended to install the liquid redistributors at regular intervals along the column height.

There is only a limited number of papers devoted to experimental investigations of flow distributions over the column cross-section. The most common method to study the liquid maldistribution is liquid collection under the packing by the fixed or movable headers.[6,21–26] Application of some methods based on x-ray computer tomography and gamma-tomography for flow investigation in packing with catalysts and structured packing are known in literature as well.[11,16,27,28] These methods are aimed at the measurement of liquid distribution on the packing and its accumulation inside the packing, though they do not provide information on the local composition of mixture. Distribution of water flow with the counter-current vapor flow in the column of 0.3-m diameter was studied by Gunn and Al-Saffar[21] on different types of irregular packing. The packing height was varied from 0 to 1.75 m. To measure the local flow rate distribution under the packing, four ring headers are used. Liquid distribution over the cross-section depends on wettability of the packing material and initial nonuniformity of irrigation. According to the measurements, up to 60% of liquid is in the near-wall zone. The spreading coefficients of water flow for the irregular and structured packing in the hydraulic simulator of the 0.5-m column were determined by Hoek et al.[22] Most studies are devoted to the effect of nonuniform liquid distribution as it is assumed that vapor maldistribution slightly effects separation efficiency.[29] Controlled maldistribution at the column inlet at mixture separation was studied by Olujic and Graauw[23] and Pavlenko et al.[6] Experiments[23] on separation of methanol–ethanol mixture were carried out in the column of 0.45-m diameter on two types of the packing with specific surface areas of 250 and 500 m^2/m^3. It was shown that the shape of initial distribution has a significantly greater effect on separation efficiency than the drip point density. The packing with higher specific surface area is strongly influenced by the initial nonuniformity. Experiments[6] were carried out in the column of the 0.9-m diameter filled with the structured aluminum packing with specific surface area of about 500 m^2/m^3 and total height of 3.3 m using the R114 and R21 mixture at the ratio of mole liquid and vapor flow rates $L/V = 1.0$ and 1.7. According to experimental results presented by Pavlenko et al.,[6] generation of initial nonuniformity of irrigation in the form of a large localized zone leads to a significant increase in liquid maldistribution inside the packing and essentially reduces the efficiency of mixture separation. At that, the development of liquid maldistribution along the column height depends on the layer turn angle. Reducing the layer turn angle at

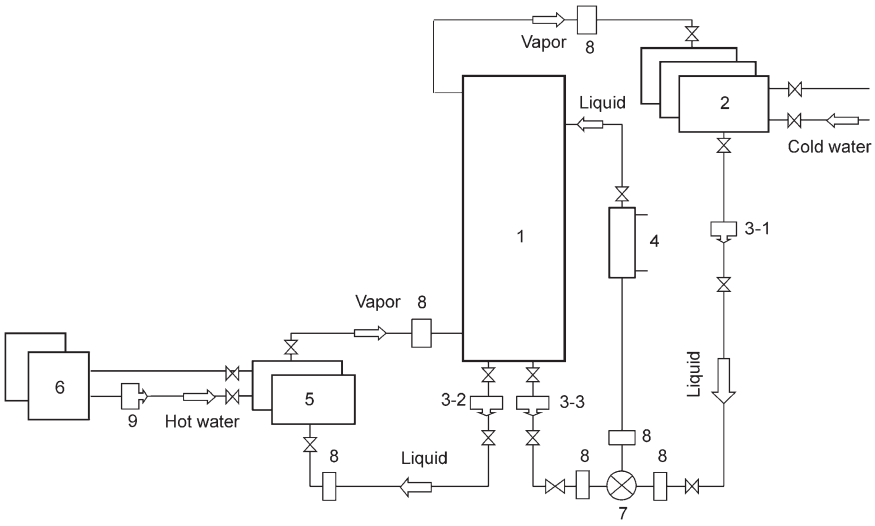

Figure 1. Technological scheme of setup "Freon Column."

1 – column; 2 – condensers, 3 piec.; 3-1, 3-2, 3-3 – freon pumps; 4 – heat exchanger; 5 – evaporators, 2 piec.; 6 – water boilers, 2 piec.; 7 – mixer; 8 – flow meters; 9 – water pump.

nonuniform packing irrigation leads to significant deterioration in the efficiency of mixture separation.

This article presents the results of experimental study on the effect of initial maldistribution of liquid, specified by the distributor holes pattern, on the parameters of the counterflow, and efficiency of Freon mixture separating on the 19-layer Mellapak 350.Y structured packing. This article presents the results of experimental investigation on parameters of the large-scale maldistribution of mixture composition and local flow over the packing cross-section and the column wall. Distributions of mixture composition are determined via the measurements of temperature field over the cross-section inside the packing and temperature field and concentration under the packing.

Experimental Setup and Investigation Methods

Experiments were carried out on the setup "Freon column." The scheme of setup shown in Figure 1 was described in detail in Pavlenko et al.[25,26] The setups operated by the closed cycle. Vapor from the upper part of the column (1) is sent to shell-and-tube condensers (2), where it is condensed by cooling water. Liquid from condensers is fed by pump (3-1) through heater (4) to the liquid distributor located in the upper section of the column (1). Liquid from the column is sent by pump (3-2) to evaporators (5). Liquid boils due to the heat of hot water, which is heated in the circuit of electric heaters (6). Vapor from the evaporators is sent to the vapor distributor in the lower part of the column. When the setup operates at liquid to vapor ratio $L/V > 1$, additional liquid from the lower part of the column is fed to the liquid flow from condensers by pump (3-3). These two flows mix in mixer (7) and they are sent to the liquid distributor of the column. The working mixture from the circuit is removed by the pumps and via evaporation of residual liquid by the heater on the column bottom. Before column disassembling, residual vapors are condensed by the refrigerating machine. At evacuation, the working mixture is pumped from the setup into the storage vessels. After column assembling just before filling with a refrigerant, the air is pumped out of the column by the vacuum pumps. The separation column with the inner diameter of 0.9 m and height of 6.8 m consists of nine sections. The vapor predistributor is mounted in the lower section. In the lower measurement section, there is the system for measurement of local characteristics with the mechanisms of probes' transportation over the column cross-section. The vapor distributor in the form of the sieve tray with the downcomers is also mounted in the lower measurement section. Parameters of the sieve tray at its fabrication were chosen to ensure no flow of liquid through its holes and achieve minimal droplet removal from the surface of the bubble layer within the specified range of liquid and vapor flow rates in accordance with recommendations on the design of bubble sieve trays. According to visualization, in the studied range of liquid and vapor flow rates, there are no both liquid flow through the sieve tray at low vapor and liquid loads and visible droplet removal from the surface of two-phase bubble layer on the tray at high liquid and vapor loads. The scheme of vapor inlet and distribution in the lower part of the column is shown in Figure 2. The pipelines for vapor and liquid inlet and outlet are located on the lateral side of the head and lower sections of the column. Vapor through halfpipe (1), cut from the bottom, is sent to vapor volume (2). On the lid of vapor predistributor (2), there are 452 pipes (3) with the height of 0.1 m and diameter of 0.01 m for leveling the streamlines and preliminary uniform distribution of vapor over the column cross-section. Then, vapor passes through sieve tray (4) with bubble two-phase layer (5) and comes to structured packing (6). The lower packing layer is supported by grid (7), mounted in the upper cross-section of the measurement section. Liquid from the lower edge of the packing falls on the sieve tray (Figure 3), and then across the overflow rims it follows to the tray downcomers (8). The distance between the packing and sieve tray is 0.416 m. To exclude the contact between liquid from the sieve tray and incoming vapor, liquid is evacuated by drainage tubes (9) from the downcomers to the lower part of the column. Liquid from the column is removed via pipe (10).

There are four windows of 60-mm diameter for visualization in the measurement sections; in the packing sections, there two windows in each. 1, 2, 4, 5, and 8 packing layers in any combination can be mounted in the packing sections

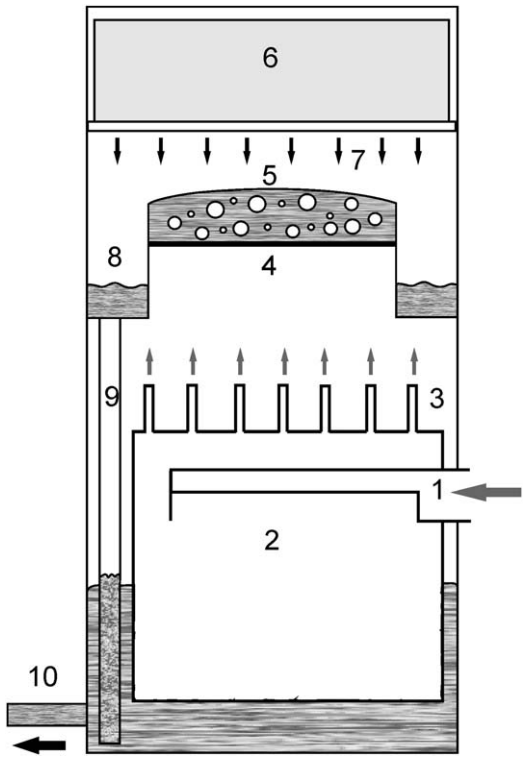

Figure 2. The scheme of vapor inlet.

1 – vapor inlet; 2 – vapor volume; 3– tubes for vapor outlet from the predistributor; 4 – sieve tray; 5 – two-phase layer; 6 – structured packing; 7 – supporting grate; 8 – downcomers; 9 – drainage tubes, 2 piec.; 10 – liquid outlet.

at different heights. All sections of the column, excluding the bottom and the head ones can be installed in any order by height. The packing height in the column can vary from 0.2 to 4 m.

The packing was irrigated by the distributor with drip point density of 131 m^{-2}. The distributor is a tank of 0.5-m height. The channels for vapor removal are welded into the tank bottom. The ratio of the area of vapor passage cross-section to the area of column cross-section is $\approx$40%. To achieve the given drip point density, there were 83 nozzles in the distributor bottom with the hole diameter of 5 mm. In this liquid distributor, there was the rectangular drip point pattern (see Figure 4). The steps between distributor holes and the angle of distributor installation are chosen to achieve most uniform wetting of the packing in longitudinal and transverse directions. Liquid is fed into the distributor through a horizontal tube predistributor with the holes on lateral generatrices. The predistributor is mounted at the height of 0.2 m above the distributor bottom. The working range of hydrostatic level above the holes of liquid distributor changes from 0.05 to 0.48 m. According to water testing of liquid distributor and predistributor, nonuniformity of jet flow rate over the cross-section did not exceed 3% in the whole studied range of liquid flow rates. With a single liquid jet impinging on the upper packing layer at the layer outlet, the wetted zone extending in the direction of the packing sheets is formed because liquid spreading along the sheets is substantially higher than in the transverse direction.[22] At a small turn angle of the underlying layer at its outlet, the extending wetted zone will be formed in the direction of the

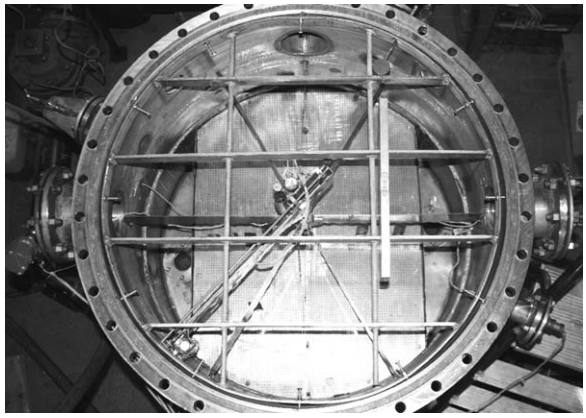

Figure 3. Sieve tray in the column.

packing sheets. At the large turn angle, a wider wetted zone is formed. Thus, varying the angle of the layers, it is possible to influence the characteristics of liquid distribution in a structured packing. In this work, the experiments were carried out at the layer turn angle of 90°. Maldistribution of the local liquid flow rate over the packing cross-section is created by closure of one or two rows of holes in the bottom of distributor. There are two rows of holes in the bottom of the distributor with eight nozzles in each, which can be tightly closed independently by means of devices managed outside of the column operating under the conditions of mixture separation. This construction allows the experiments with initial nonuniformity of packing irrigation of about 10% (one blocked row) and 20% (two blocked rows). The scheme of row blocking is also shown in Figure 4. The liquid distributor was mounted at the distance of 135 mm from the upper

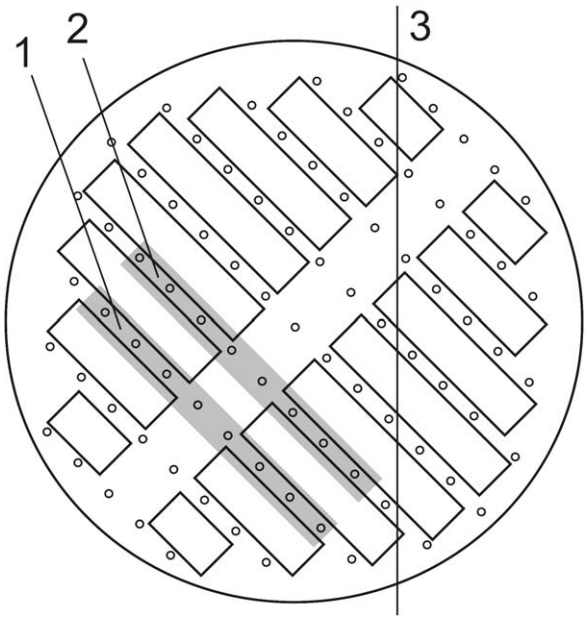

Figure 4. Location of liquid distributor relative to the packing.

The following topograms of local parameters distribution over the column cross-section are shown in the same coordinate system. 1 – row No. 1 is blocked; 2 – row No. 2 is blocked; 3 – orientation of packing sheets in the upper layer.

packing layer. The rows of holes on liquid distributor were located at 45° relative to the direction of the sheets in the upper packing layer. The experiments were carried out on the mixture of R114 (dichlorotetrafluoroethane—$CClF_2$-$CClF_2$) and R21 (dichlorofluoromethane—$CHCl_2F$) freons at the ratio of mole flow rates of liquid and vapor $L/V = 1.0$ and 1.7. Freon R114 in this mixture is the volatile component. The experiments were carried out at the absolute pressure in the upper part of the column $p_{top} = 3$ bars. The composition of separated mixture was chosen experimentally to avoid extremely low volatile concentration at the column bottom and not to achieve the azeotropic point at the column top. The azeotropic point for R21/R114 mixture is 62.22%. All experiments, results of which are presented in this article, were carried out in the range of concentrations of volatile component R114 from 0 to 60%, that is, to the left from the azeotropic point. Mixture concentration in the column bottom under the sieve tray was kept constant in all experiments and it was 0.3%. In experiments at $L/V = 1$ vapor concentration at the packing outlet and liquid concentration at the inlet did not exceed 56% at a change in regime parameters. In experiments at $L/V = 1.7$ vapor concentration at the packing outlet and liquid concentration at the inlet did not exceed 15 and 8%, respectively. Under these conditions the difference between vapor concentration at the equilibrium line and measured value $(y_e - y_{top})$ at $L/V = 1.7$ does not exceed 0.2%, and at $L/V = 1.0$, it does not exceed 1.3%. The relative measurement error for mixture concentration in vapor and liquid did not exceed 2% in the lower range of concentration change, and it was not higher than 0.2–0.5% in the upper part of the column. Finally, the maximal relative error in determination of height, equivalent to the theoretical plate (HETP) parameter at $L/V = 1.0$ did not exceed $\pm 1.3\%$, and at $L/V = 1.7$, it was not higher than $\pm 2.7\%$.

The structured Mellapak 350.Y packing of stainless steel 316L with specific surface of about 350 m^2/m^3 was mounted in the column. The total packing height was 4.016 m. To reduce liquid accumulation on the column wall, each layer had two rows of wipers made of stainless steel gauze on the lateral side. The packing sheets were perforated. Packing microtexture was made in the form of projections. The average gap between the column wall and lateral side of the packing was 10.0 mm. In the lower part of the column, there was the measurements section with the system for measurement of local liquid flow rates and concentrations at the packing outlet. Distribution of the local flow rate density of liquid in the column cross-section at the packing outlet was measured by specially designed low-head flow meter installed on a two-coordinate device, which allowed programmed scanning of the column cross-section. The scheme and operation principle of the low-head flow meter are described in detail in Serov et al.[30] There was also the liquid sampler on the two-coordinate device, and a sample was sent to the chromatograph through this sampler to measure the composition of two-component mixture. The flow meter was positioned in the column cross-section with accuracy of ± 1 mm along the radial and azimuth coordinates by means of two independent electric drives. The local flow rate was measured at 419 points, distributed uniformly over the column cross-section. The pattern of point location is shown in Figure 5. The flow meter includes the round receiving collector with the diameter of 28 mm and the jets from the packing flow into this collector. After every experiment, the flow meter is calibrated using the same liquid and under the same conditions as in the experiment.

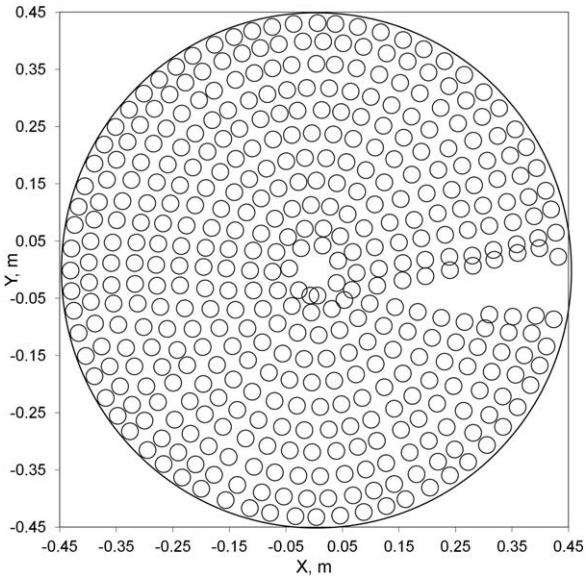

Figure 5. The scheme of scanning points in the column cross-section at the packing outlet.

This system allows us to analyze the effect of initial maldistribution of packing irrigation on distribution of the local flow rate and liquid concentration at the packing outlet at a change in different parameters. In particular, the effect of the packing layers' number on distribution of local flow rate and concentration of liquid over the cross-sections of different packing and over the column wall at uniform and nonuniform irrigation was shown in Pavlenko et al.[6,10,25,26] using the given measurement system.

First, there was the experimental series at uniform packing irrigation, then, we have performed the experiments at nonuniform irrigation, keeping all external conditions and operation parameters. During the experiment, the following operation parameters were changed: volumetric vapor flow rates at the column inlet and outlet; volumetric flow rate of liquid fed to the evaporators; volumetric flow rate of liquid at the column inlet; pressure in the column, condensers, and evaporators; flow rate of hot water fed to the evaporators and the flow rate of cold water fed to the condensers; water temperature at the inlet and outlet of evaporators and condensers. The composition of vapor and liquid mixture at the column inlet and outlet was measured by the method of gas chromatography. Velocities of liquid and vapor were determined via division of volumetric flow rates by the area of column cross-section. The volumetric vapor flow rate was measured by the flow meter mounted on the pipeline for vapor removal from the column head to the condensers. The volumetric liquid flow rate was measured by the flow meter mounted on the pipeline supplying liquid to the distributor located in the column head. The pressure in the column and in other parts of setup was measured by the pressure probes Metran-100. The pressure drop on the packing was measured by the differential pressure probe Metran 150-DD. Physical properties required for calculation of all parameters were calculated by the measured pressure and mixture composition at corresponding points. Experimental data on mixture separation and pressure drop are presented depending on the generalized parameters calculated for the upper part of the column

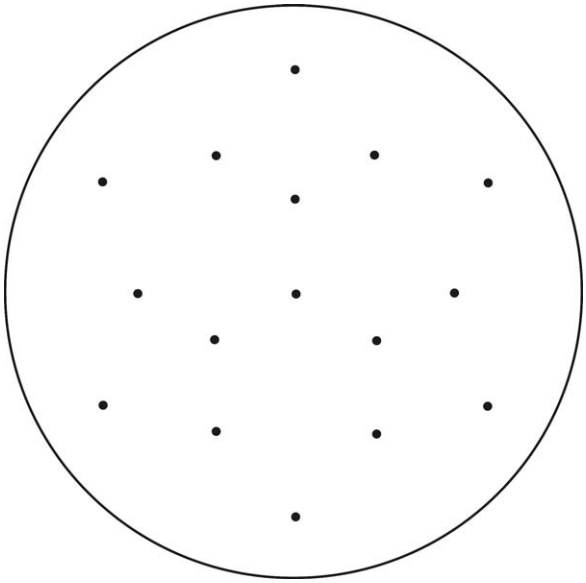

Figure 6. The layout of 16 thermal sensors in the packing layer.

according to the common practice of data presentation in the field of distillation.

To measure distributions of the local mixture composition in a cross-section inside the packing, we have used the method based on the measurement of temperature fields. The temperature sensors were mounted inside the packing within one cross-section. There were 16 sensors in this cross-section. Distribution of mixture composition in the packing cross-section was calculated by temperature measurements on the basis of equilibrium concentration at the given temperature. The detailed description of this measurement method is shown in Pavlenko et al.[10]

The silicon diodes KD512 were used as the temperature sensors. These silicon sensors have good time stability, small sizes (the frameless devices are smaller than 1 mm), high sensitivity (about 2 mV/°C). Implementation of the commutation scheme on the diodes with one-way conductivity allowed reduction in the number of measurement lines. The thermometers were calibrated together with the connecting lines. The thermostat Thermo Haake DC-30 was used for calibration; it ensures the stability of temperature maintenance of 0.02°C. Our developed scheme of temperature measurements allows registration of temperature change with accuracy not worse than 0.05°C. The thermal sensors were mounted inside the structured packing at the level of the sixth layer from the packing bottom. Sensors location along the column height and over the cross-section is shown in Figures 6 and 7. Inside the packing, these sensors were mounted in the corners of the channels formed by adjacent corrugated sheets of the packing. This location was chosen after special experiments on visualization of the character of the liquid flow in the packing in a wide range of liquid load. According to results of these experiments, in the corners of channels formed by adjacent corrugated sheets of the packing we can observe the intensive flow and mixing in the falling liquid film with almost 100% probability. This is also proved by results of Alekseenko et al.,[7] where distributions of film thickness in channels of the structured packing were measured using the fiber-optic probes. Therefore, the position and size of the applied thermal sensors are determined by the conditions of temperature distribution measurements in the falling liquid phase. A thermal sensor was also mounted under the packing on the two-coordinate device. This sensor is located in the receiving collector of the chromatograph sampler and it was dipped into the liquid running from the packing.

Distribution of liquid concentration over the column cross-section at the packing outlet was measured by two methods. The first method was the direct measurement of mixture composition via the chromatographic analysis. The liquid from the packing also flowed to the collector of 30-mm diameter. Another method was based on the measurement of liquid temperature and pressure under the packing. The liquid temperature was measured in the collector made for taking samples from the chromatograph. Liquid concentration was calculated by these data using dependences $C=f(P,T)$ at the line of equilibrium.

Thus in our experiments, we have measured distribution of temperature fields in two cross-sections of the column. Distributions of mixture composition were calculated by the

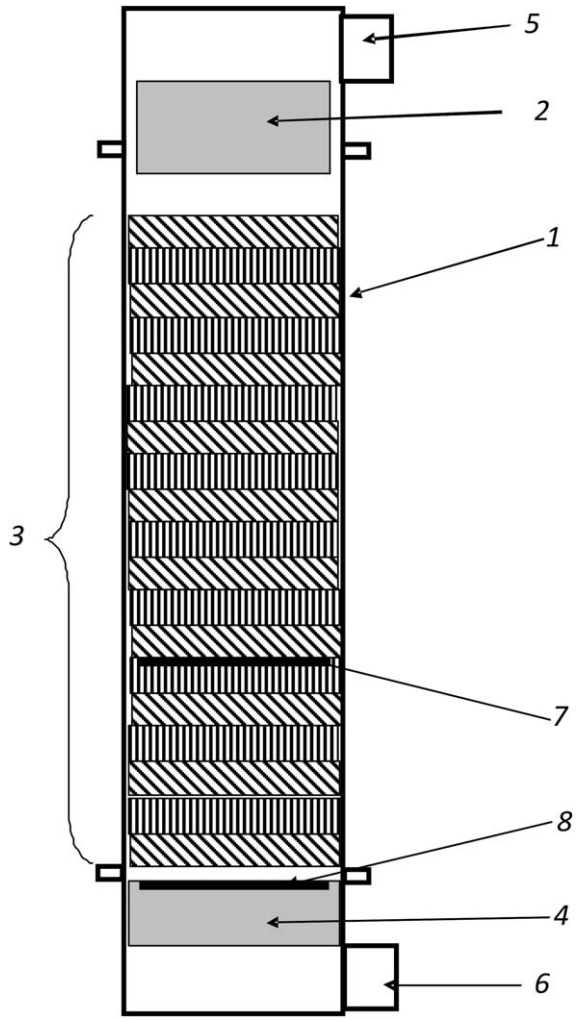

Figure 7. Location of temperature sensors over the column height.

1 – column shell; 2 – liquid distributor; 3 – structured packing; 4 – measurement section; 5 – thermometer in liquid pipeline at the column inlet; 6 – thermometer in liquid pipeline at the column outlet; 7 – thermometers in the sixth packing layer (16 pieces); 8 – thermometer on two-coordinate device.

temperature fields using the properties of R21-R114 mixture under the equilibrium conditions for the given pressure. Calculations for cross-sections inside the packing and under the packing were made at the assumption that the temperature was measured in the liquid phase. The pressure in the column was measured under and above the packing. The pressure inside the packing at every level was determined through linear interpolation of the pressure drop on the packing. Distributions of local flow rates and concentrations of liquid over the cross-section are shown as topograms. All topograms of local parameters' distribution over the column cross-section are shown in the same coordinate system as the liquid distributor in Figure 4.

Experimental Results and Discussion

Experimental data on separation efficiency and pressure drop

Efficiency of mixture separation in the column [height of transfer unit (HTU) and HETP] is calculated by the measured mixture composition in the vapor and liquid phases at the column inlet and outlet and equilibrium data. In the bottom of the column, the mixture is separated within the bubble layer on the sieve tray as well as on the liquid jets in space between the lower plane of the packing and the sieve tray (Figure 2). To determine the sieve tray contribution to the total mixture separation in the column, we have performed the experiments on mixture separation in the column without packing. There were the liquid distributor and the sieve tray mounted in the column. The distance between them in this experimental series equaled the distance between the liquid distributor and the packing plus the distance between the packing and the sieve tray. The mixture was separated within the bubble layer on the sieve tray and on the liquid jets flowing from the distributor. The number of theoretical stages of separation were calculated by measurement results on mixture composition in the vapor and liquid phases at the column inlet and outlet within the working range of liquid and vapor flow rates at $L/V = 1$ and $L/V = 1.7$. According to results of these experiments, the contribution of total mass transfer on the sieve tray and liquid jets from the single packing channels depends weakly on the vapor and liquid loads within the studied range, and mixture separation corresponds to ≈1.1 of the theoretical stage. It was assumed that separation efficiency on the sieve tray does not depend on the vapor flow rate. On the basis of these estimates, concentrations of the volatile component in the vapor and liquid phases directly under the packing $x_{\text{pack}}^{\text{bot}}$ and $y_{\text{pack}}^{\text{bot}}$ were calculated, these values were used for calculation of HTU and HETP values on the structured packing of the given height.

Data on separation efficiency at uniform packing irrigation at the inlet are shown in Figure 8 depending on the mole flow rates of vapor and liquid phases at different L/V parameters. In experiments with total reflux ($L/V = 1$) at low vapor flow rates, starting from $F_v \approx 1.2$ Pa$^{1/2}$, the HETP value increases drastically with a decrease in the vapor flow rate and, respectively, with a decrease in the liquid flow rate. This may be caused by the deficit of liquid because at relatively low drip point density set in experiments some sheets stay dry. According to experiments of Pavlenko et al.[8] on the single elements of the structured packing at low liquid flow rates, the film flow inside the channels loses the continuity, and the rivulet flows with formation of dry spot, reducing the real mass-transfer surface, become predominant. At low liquid flow rates, its main portion flows along the corrugation channels, and the flow across the ribs is insignificant. In this case, even the contact points (the points of contact between the crests of adjacent packing sheets) do not ensure the sufficient transfer of liquid in transverse direction on the every packing layer. At vapor flow rates corresponding to $F_v \geq 1.2$ Pa$^{1/2}$, and higher liquid flows, when the packing becomes wetter, the value of HETP stays almost constant. It was shown in preliminary experiments that at $L/V \approx 2$ the difference between concentration of volatile component in the vapor phase in the column top and equilibrium concentration becomes much lesser than 0.1% because of the high separation efficiency on 19 installed packing layers, therefore, the number of theoretical separation stages is determined with a large error. Finally, inclination of the operating line was chosen $L/V = 1.7$. With an increase in the ratio between liquid and vapor flow rates the value of HETP decreases drastically and stays almost constant in the whole studied range. No significant increase in HETP values at low values of the parameter F_v in experiments with $L/V = 1.7$ is explained by better wetting of the mass-transfer surface. It can be seen from Figure 8b that in experiments with $L/V = 1.7$ the relative liquid flow rates at $w_L > 3.1 \times 10^{-3}$ m/s correspond to the plateau area for the experiments at $L/V = 1$, where the effect of dry spots on separation efficiency is insignificant. Results of pressure drop measurements on the packing are shown in Figure 9. Here, we show the measured pressure drop reduced to the total height of the

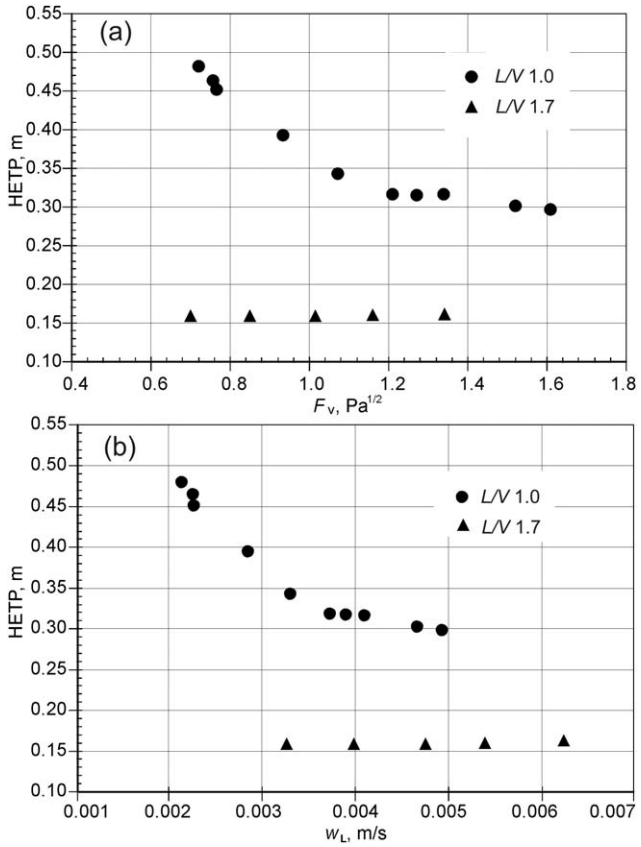

Figure 8. Efficiency of Freon mixture separation (HETP) on the Mellapak 350.Y packing at uniform irrigation.

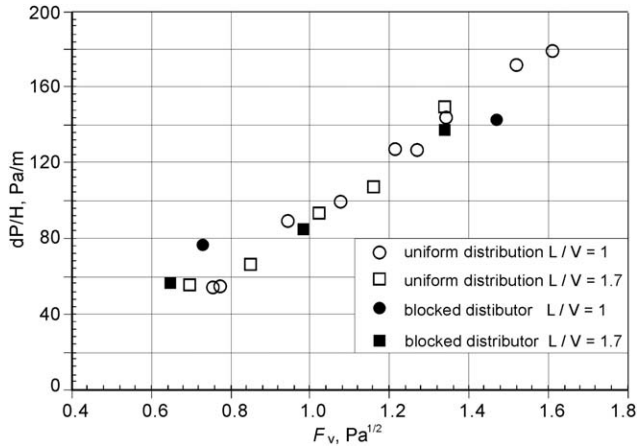

Figure 9. Relative pressure drop on the Mellapak 350.Y packing at uniform and nonuniform liquid irrigations.

packing. Under the experimental conditions an increase in L/V from 1 to 1.7 does not effect the relative pressure drop on the packing at uniform liquid irrigation at the packing inlet. The pressure drop is determined by the vapor flow rate. On the studied structured packing with specific surface of 350 m^2/m^3 the hydraulic diameter of channels is ≈11.6 mm, therefore, an increase in the film thickness at an increase in L/V does not effect significantly a decrease in the flow area of vapor and does not lead to an increase in hydraulic resistance.

Experimental data obtained at nonuniform irrigation at the packing inlet are shown below. As it was shown in Figure 4, both blocked rows of holes are located alongside, in one half of column cross-section. This is made to concentrate the zone of maldistribution in one area at its increase, and do not spread it uniformly over the column cross-section. Otherwise, the effect of maldistribution would be reduced to the effect of drip point density at symmetrical blocking relative to the center. To estimate qualitatively the degree of maldistribution Lockett and Billingham[31] have introduced maldistribution coefficient f_{max}. The critical values of maldistribution coefficient, when mass transfer deteriorates, can be determined according to Ref. 31 by relationship:

$$f_{max} = \frac{y_e - y_{top}}{y_{top} - y_{bot}} + \frac{x_{bot} - x_e}{x_{top} - x_e} - \frac{y_e - y_{top}}{y_{top} - y_{bot}} * \frac{x_{bot} - x_e}{x_{top} - x_e}, \quad (1)$$
$$y_e = f(x_{top}), x_e = f(y_{bot}).$$

To determine this coefficient, we should know only the compositions of vapor and liquid phases at the column inlet and outlet, which can be achieved via the experiment or calculation on separation efficiency of the column. If the real maldistribution coefficient at the packing inlet is $f > f_{max}$, we will observe a decrease in separation efficiency in comparison with the calculated one. The suggested analysis is based on the very approximated model for two parallel columns, where the ratios of liquid and vapor flow rates deviate from the averaged flow rates for the whole cross-section. At significant maldistribution of irrigation and large packing height concentrations at the ends of the operating line in every column approximate the equilibrium values, and the process of separation in the zone of convergence stops because of zero concentration difference. At $(y_e - y_{top}) \to 0$ or $(x_{bot} - x_e) \to 0$, we can observe the so-called pinch effect. For the local operating line at an increase in L/V this effect is shown in the upper part of the column, and for the operating line with a reduced value of L/V it is shown in the bottom part. Due to the pinch effect in any of parallel columns their total efficiency decreases in comparison with the column with uniform irrigation. The degree of efficiency reduction depends on the calculated number of theoretical separation stages. According to the analysis of calculation results by Ref. 31 Figure 10, the higher the number of theoretical stages of separation, the stronger the efficiency decrease. At a small column height (low number of theoretical stages) more significant initial maldistribution is accepted without a loss of efficiency.

For $L/V = 1$ within the HETP plateau $f_{max} = 0.031$, for $L/V = 1.7$ $f_{max} = 0.033$. Initial maldistribution of 10 and 20%, set at the inlet, are higher than the critical value of the maldistribution criterion cited in Lockett and Billingham,[31] therefore, we can expect separation deterioration in experiments with blocking the distributor zones indicated in Figure 4. Data on efficiency of mixture separation obtained in experiments with initial maldistribution of irrigation at $L/V = 1$ are shown in Figure 11a for comparison with the case of uniform irrigation. It is indicated there that either the first row of holes was blocked (1) or the second row (2), or two rows simultaneously (1+2), according to Figure 4. It can be seen from these data that one row blocking leads to insignificant deterioration of separation efficiency. Generation of large maldistribution in the form of two blocked rows of holes increase the HETP, by 30–35% within the plateau. At low vapor flow rates ($F_v \approx 0.7$ $Pa^{1/2}$), the value of HETP increases approximately by 20% in comparison with uniform packing irrigation. This results agrees with the conclusions of the authors of dependence (1),[31] who showed that the lesser the number of separation stages in the column (the higher the values of HTU and HETP), the higher the critical value of coefficient of initial maldistribution. Under the given experimental conditions at a lower number of theoretical separation stages, the upper point of the operating line of the process is far from the equilibrium line, therefore, the stronger deviation of local L/V in the column from the given $L/V = 1$ is assumed without corresponding

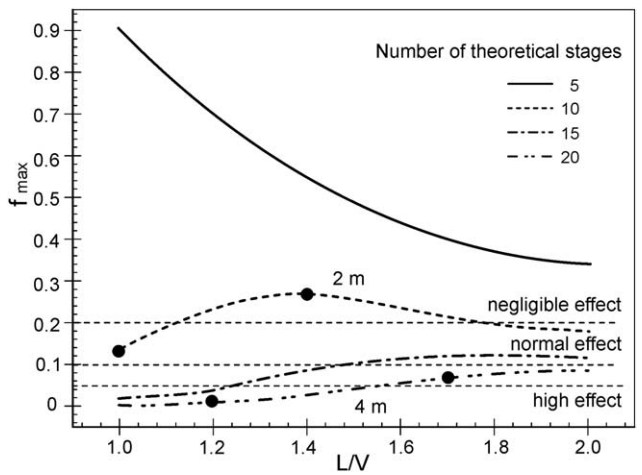

Figure 10. Dependence of limit maldistribution f_{max} of local liquid and vapor flow rates over the packing cross-section vs. the ratio of liquid and vapor flow rates (parameter L/V) at binary mixture separation.

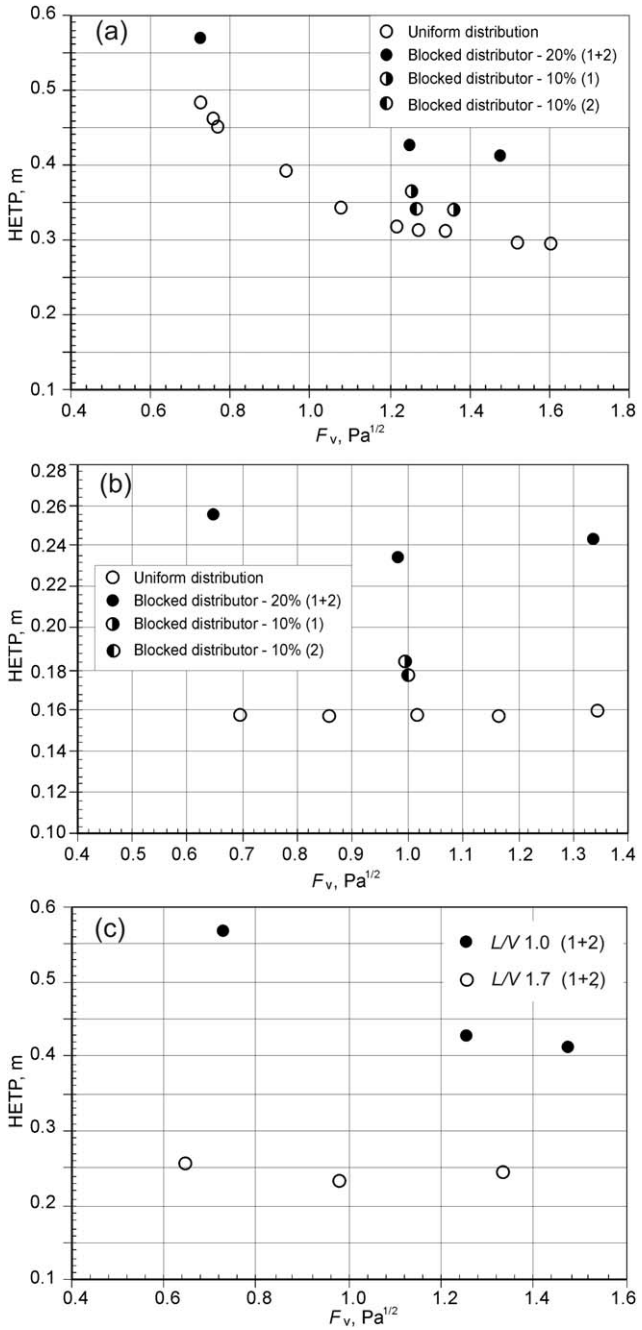

Figure 11. Efficiency of Freon mixture separation (HETP) on the Mellapak 350.Y packing at nonuniform irrigation.

deterioration of separation efficiency. Results of pressure drop measurements on the packing at initial nonuniform irrigation (simultaneous blocking of two rows: 1+2) are also shown in Figure 9. Data on hydraulic resistance depend weakly on uniformity of packing irrigation.

Experimental results on the effect of initial nonuniformity of packing irrigation at $L/V = 1.7$ are shown in Figure 11b. The value of HETP in experiments with initial nonuniformity of 20% increased by 50% and more in comparison with uniform irrigation. The stronger effect of large-scale nonuniformity of irrigation in the form of two blocked rows of holes at $L/V = 1.7$ in comparison with $L/V = 1$ (by 50% as compared to 30–35%) coincides also with the conclusions of the authors of dependence (1).[31] The lesser the values of HTU and HETP, the lower the critical values of the coefficient of initial maldistribution of irrigation, which make separation worse, and the stronger the effect of this maldistribution on a decrease in separation efficiency. Blocking of one row of holes (maldistribution of about 10%) led to deterioration of separation efficiency by 10–12%. Data on separation efficiency at nonuniform packing irrigation are compared in Figure 11c for different values of L/V ratios. The character of vapor flow rate effect on HETP value stayed the same. At $L/V = 1$ with a decrease in F_v the HETP value increases. At $L/V = 1.7$, we can observe an insignificant increase in HETP at low vapor flow rates. The absolute values of HETP at $L/V = 1$ are also significantly higher than at $L/V = 1.7$. There is almost no effect of initial nonuniformity of packing irrigation on the pressure drop at $L/V = 1.7$ as at $L/V = 1$ (Figure 9).

Distribution of local parameters over the packing cross-section

In all topograms, an arrow indicates the point of vapor supply to the column. The azimuth coordinate in diagrams with data on liquid distribution on the column wall is calculated from the point located diametrically opposite to the arrow, which indicates vapor inlet. The azimuth coordinate is counted counterclockwise.

Diagrams of dependence between the portion of liquid ($q_{\text{wall rel}}$) on the wall under the packing at uniform irrigation and parameter F_v are shown in Figure 12 for $L/V = 1$ and 1.7. The portion of liquid on the wall $q_{\text{wall rel}}$ is determined as the ratio of total liquid flow rate on the wall to the total liquid flow from the column. According to the diagram, at $L/V = 1$ an increase in superficial velocity of vapor and liquid leads to an increase in the portion of liquid on the wall, whereas, at $L/V = 1.7$ the portion of liquid on the wall decreases. It can be seen that for the existing gap between the packing and column wall within the ranges of liquid and vapor flow rates achieved in experiments liquid weakly comes to the column wall. The total amount of liquid on the wall does not exceed 1.6%. According to experimental results, at nonuniform packing irrigation the distribution character and total amount of liquid on the wall at the packing outlet did not change.

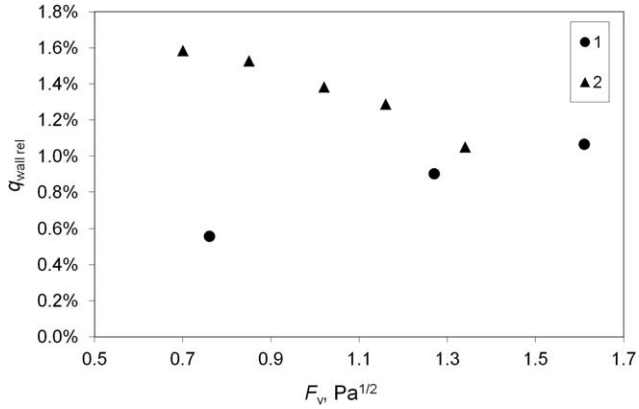

Figure 12. Diagrams of dependence between the portion of liquid flow ($q_{\text{wall rel}}$) on the wall and parameters F_v at uniform liquid irrigation.

1 – $L/V = 1.0$; 2 – $L/V = 1.7$.

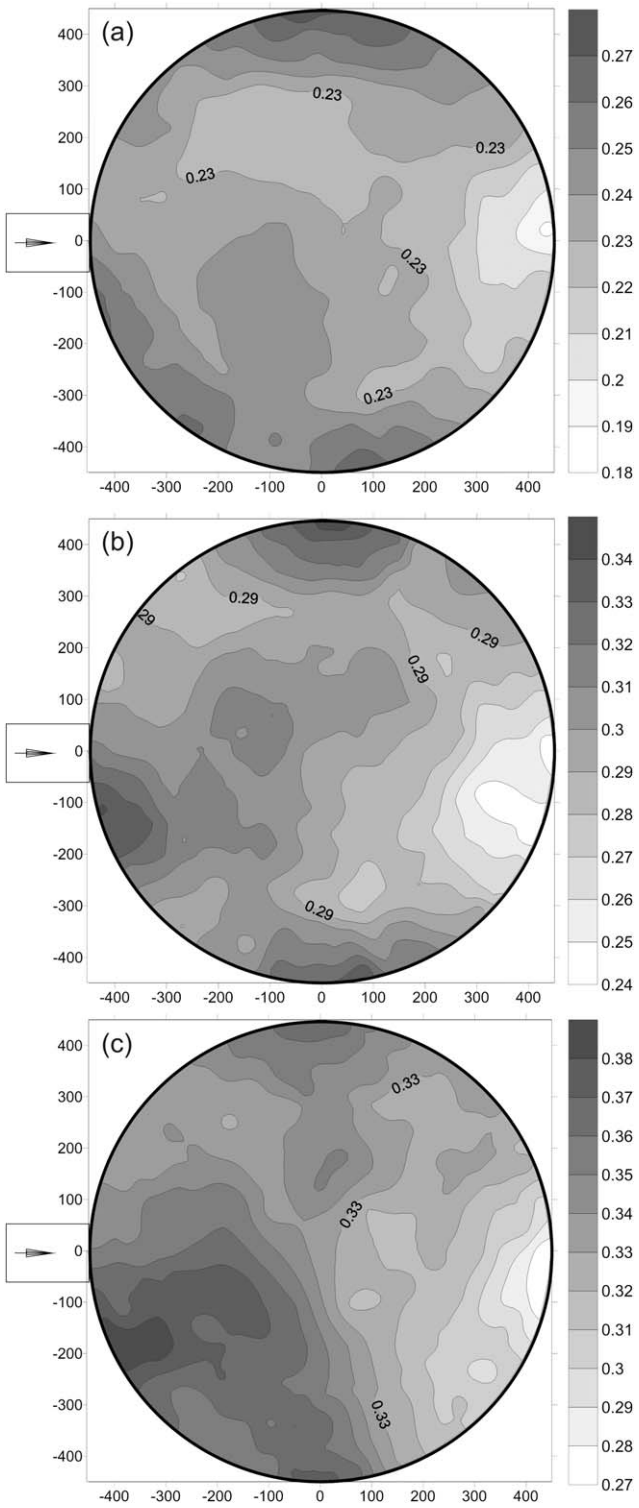

Figure 13. Distribution topograms of local density of liquid flow rate over the column cross-section under the packing at uniform liquid irrigation, 10^{-2} m^3/(m^2 s).

$L/V = 1.0$; a) -0.76; 2.25×10^{-3}; b) -1.27; 3.89×10^{-3}; c) – $Fv = 1.61$ Pa$^{1/2}$; $w_L = 4.89 \times 10^{-3}$ m/s.

As the liquid flow from the packing has the discrete character in the form of jets flowing usually from the packing corners, the number of jets coming to the measurement collector can vary within a small vicinity of measurement collector travel. To level maldistribution caused by the discrete character of liquid flow from the packing, we have performed the filtering procedure in a vicinity of every measurement point. At every measurement point, we have averaged the measured data in a vicinity of radius R. Distribution topograms for the local liquid flow rate density under the packing plotted by the measurements with averaging in a vicinity of $R = 0.114$ m are shown below.

The topograms of distribution of the local density of liquid flow rate over the column cross-section are shown in Figure 13 at column operation under the conditions of mixture separation at complete reflux ($L/V = 1$) for three values of superficial vapor velocity at uniform irrigation. According to these topograms, the distribution of local liquid flow rate is nonuniform. The zone of increased flow rate in the near-wall zone of the packing cross-section is observed up to $w_L = 3.89 \times 10^{-3}$ m/s and $F_v = 1.27$ Pa$^{1/2}$. The large-scale areas with difference of 10–15% by the flow density are observed in the central part of cross-section. Dependence of the average flow rate density of liquid in the ring cross-sections with the width of 28 mm on the ring radius at uniform irrigation is shown in Figure 14. According to the diagram, at the periphery, we can observe an increased (in the limits of 20–25%) density of liquid flow rate at $w_L = 2.25 \times 10^{-3}$ and 3.89×10^{-3} m/s. In the rest part of cross-section, the average density of liquid flow rate among the rings is relatively uniform. With a rise of w_L and F_v the increased density of liquid flow rate at the periphery decreases.

The topograms of distribution of the local density of liquid flow rate over the column cross-section are shown in Figure 15 at column operation under the conditions of mixture separation at $L/V = 1.7$ for different values of F_v at uniform irrigation. According to the topograms, distribution of local liquid flow rate is nonuniform. The area of increased flow rate is observed at the periphery and in the center of cross-section. For $w_L < 5.36 \times 10^{-3}$ m/s and $F_v < 1.16$ Pa$^{1/2}$, the zones of increased flow rate at the periphery dominate over the zone of increased flow rate in the central part of cross-section. With a rise of w_L and F_v, we observe an increase in the flow rate density in the center and its decrease at the periphery. Dependence of the average flow rate density of

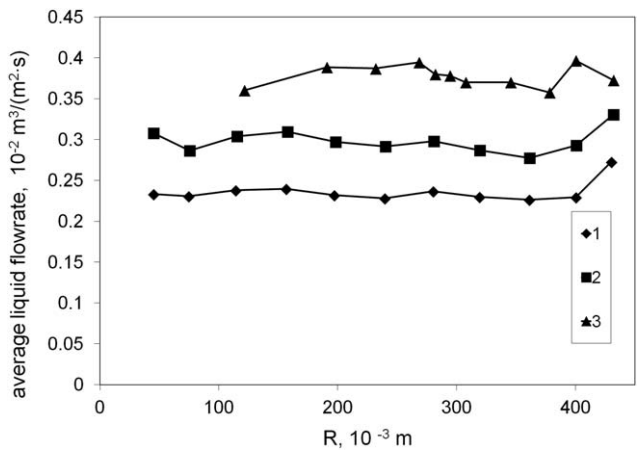

Figure 14. Dependence of average liquid flow rate density in ring cross-sections with the ring width of 28 mm on the ring radius at uniform liquid irrigation.

$L/V = 1.0$. (1, 2, 3): 0.76, 2.25×10^{-3}; 1.27, 3.89×10^{-3}; $F_v = 1.61$ Pa$^{1/2}$, $w_L = 4.89 \times 10^{-3}$ m/s.

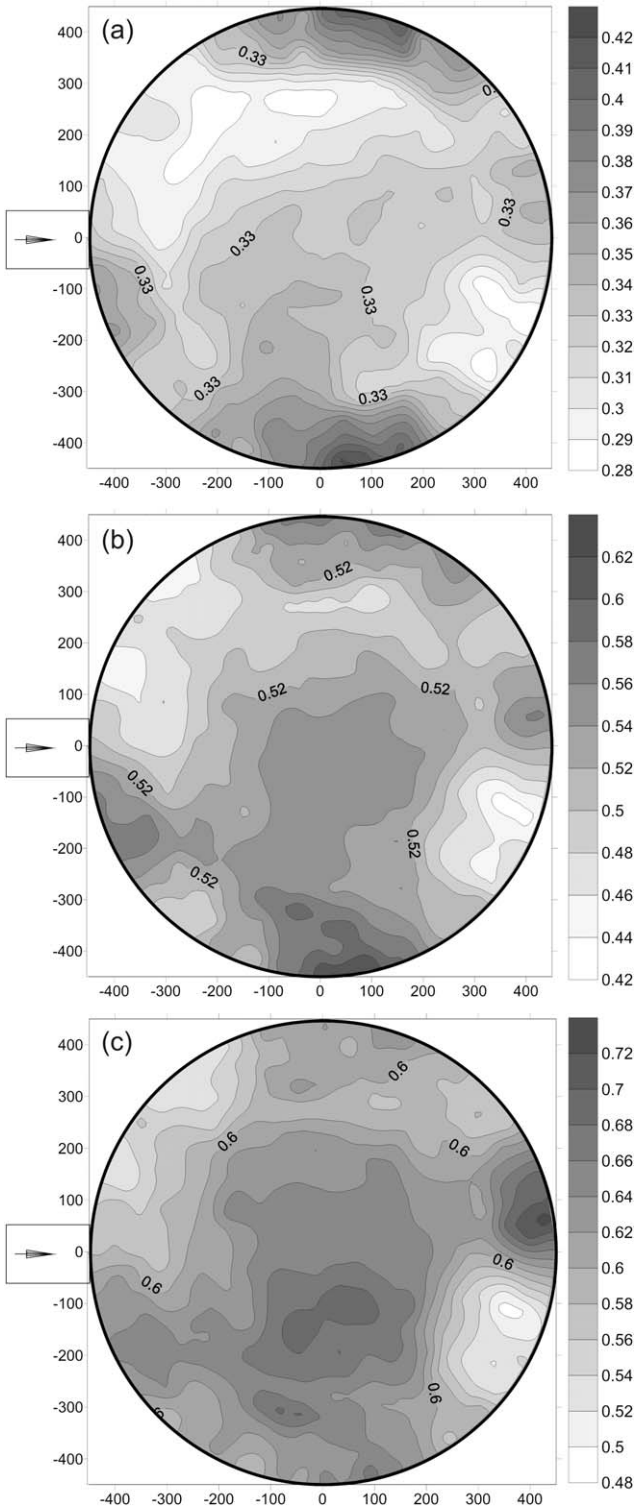

Figure 15. Distribution topograms of local density of liquid flow rate over the column cross-section under the packing at uniform liquid irrigation, 10^{-2} m^3/(m^2 s).

***L*/*V* = 1.7; a) – 0.70, 3.25 × 10^{-3}; b) −1.16, 5.36 × 10^{-3}; c) – F_v = 1.34 Pa$^{1/2}$; w_L = 6.19 × 10^{-3} m/s.**

liquid in the ring cross-sections with the width of 28 mm on the ring radius at uniform irrigation is shown in Figure 16. As it can be seen in the diagram, at $w_L = 3.25 \times 10^{-3}$ m/s and $F_v = 0.70$ Pa$^{1/2}$ the increased density of liquid flow rate (in the limits of 20–25%) is observed at the periphery,

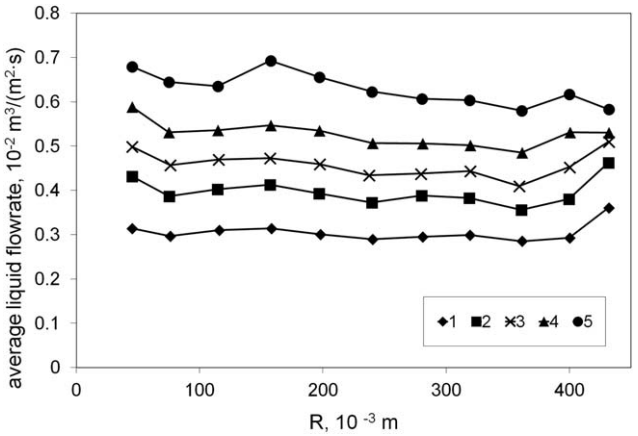

Figure 16. Dependence of average liquid flow rate density in ring cross-sections with the ring width of 28 mm on the ring radius at uniform liquid irrigation.

***L*/*V* = 1.7. (1–5) – 0.70, 3.25 × 10^{-3}; 0.85, 3.97 × 10^{-3}; 1.02; 4.72 × 10^{-3}; 1.16, 5.36 × 10^{-3}; – F_v = 1.34 Pa$^{1/2}$; w_L = 6.19 × 10^{-3} m/s.**

whereas in the rest part of cross-section we can observe almost uniform distribution of the average density of liquid flow rate within the rings. With a rise of w_L and F_v up to 4.72 × 10^{-3} m/s and 1.02 Pa$^{1/2}$, respectively, we can observe an increase in the liquid flow rate density toward the center of cross-section with constantly increased flow rate at the periphery. The following increase in parameters w_L and F_v leads to reduction in the average density of liquid flow rate within the peripheral ring to the minimal value in cross-section and enlargement of the liquid flow rate in the center of cross-section.

According to topogram analysis, nonuniform packing irrigation did not lead to any significant changes in the

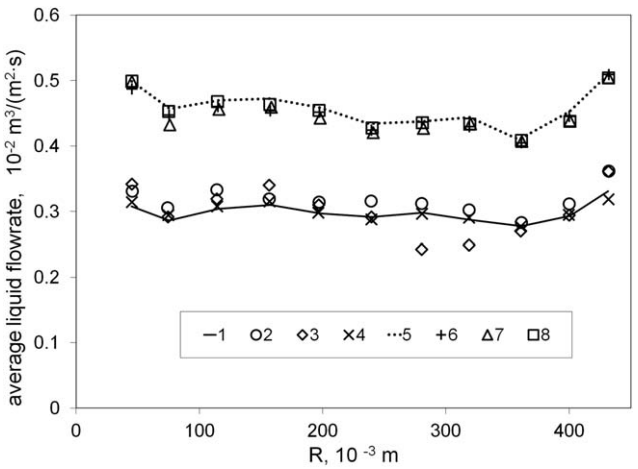

Figure 17. Average liquid flow rate density in the ring cross-sections of the 28 mm width vs. ring radius.

***L*/*V* = 1.0: 1- No blocking; 1.27; 3.89 × 10^{-3}; 2- Row No. 1 is blocked; 1.25; 3.78 × 10^{-3}; 3- Row No. 2 is blocked; 1.27; 3.86 × 10^{-3}; 4- Rows No. 1, 2 are blocked; F_v = 1.25 Pa$^{1/2}$; w_L = 3.75 × 10^{-3} m/s; *L*/*V* = 1.7: 5- No blocking; 1.02; 4.72 × 10^{-3}; 6- Row No. 1 is blocked; 1.0; 4.61 × 10^{-3}; 7- Row No. 2 is blocked; 1.0; 4.64 × 10^{-3}; 8- Rows No. 1, 2 are blocked; F_v = 0.98 Pa$^{1/2}$; w_L = 4.58 × 10^{-3} m/s.**

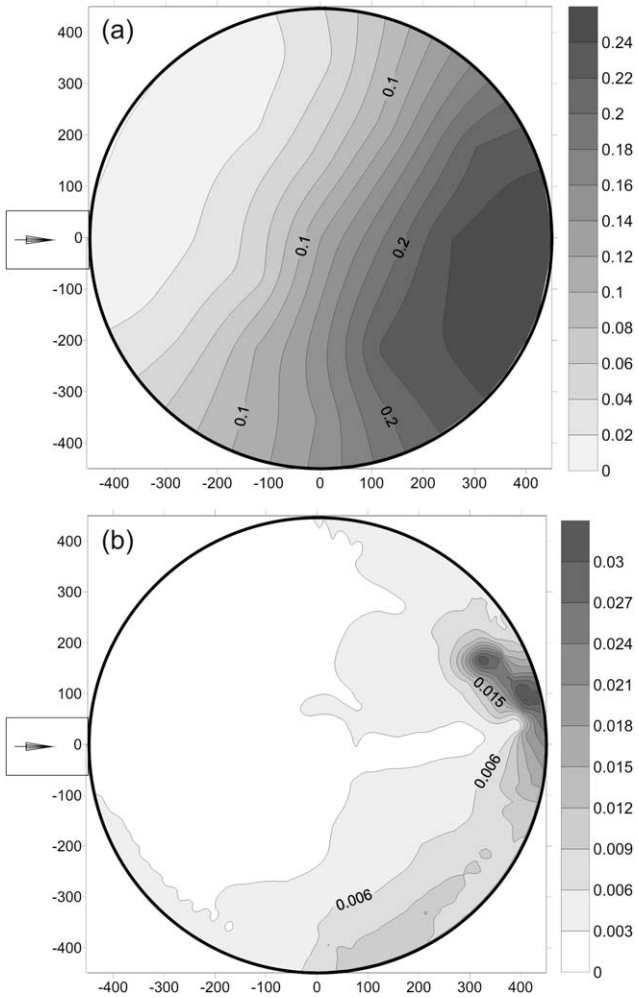

Figure 18. Distribution topograms for local concentration in column cross-section at the level of the sixth packing layer (a) and under the packing (b) at uniform liquid irrigation.

$L/V = 1$. $F_v = 1.27$ Pa$^{1/2}$; $w_L = 3.89 \times 10^{-3}$ m/s.

character of distribution of the local liquid flow rate at the outlet of 19-layer packing at corresponding vapor loads for both values of L/V. Distributions of density of the local liquid flow rate within the ring cross-sections at uniform irrigation and different versions of distributor hole blocking are compared in Figure 17. As it can be seen in the diagram, in case of $L/V = 1$ we observe a 15% decrease in the flow rate density in a vicinity of ring zones of $R = 0.30$ m at blocking zone No. 2. In other case differences of distributions are insignificant. At $L/V = 1.7$, when more liquid flows over the packing, generation of nonuniformity at packing irrigation was not detected by the analysis of average liquid flow rate density within the ring cross-sections at the packing outlet.

According to analysis of readings of 16 temperature sensors, mounted inside the packing at the level of the sixth layer at transition to stationary column operation, during the initial period the temperature was almost uniform over the cross-section. When some degree of mixture separation is achieved, instability of the counter-current flows develops in the packing, and then the stationary fields of temperature and concentration distributions with the stable profiles of these parameters nonuniformity over the column cross-section are formed.

The typical distributions of concentration over the packing cross-section at the level of the sixth layer and distributions of liquid concentration over the column cross-section under the packing at uniform irrigation of the packing inlet are shown in Figures 18 and 19. It can be seen in these figures that distributions of liquid concentration in the packing and under it are significantly nonuniform over the cross-section. The diametrically opposite areas with minimal and maximal concentrations are observed there. The positions of areas with minimal and maximal concentration almost coincide in the cross-section of the sixth layer and in the column cross-section under the packing. The fields of liquid concentration distribution under the packing plotted by temperature measurements at 419 points of column cross-section match the fields plotted by 16 temperature measurements inside the packing. The concentration gradient directed diametrically from the area of minimal concentration to the area of maximal concentration is obvious. As we can see in the typical figures, considerable temperature maldistribution over the packing cross-section is observed. This maldistribution has

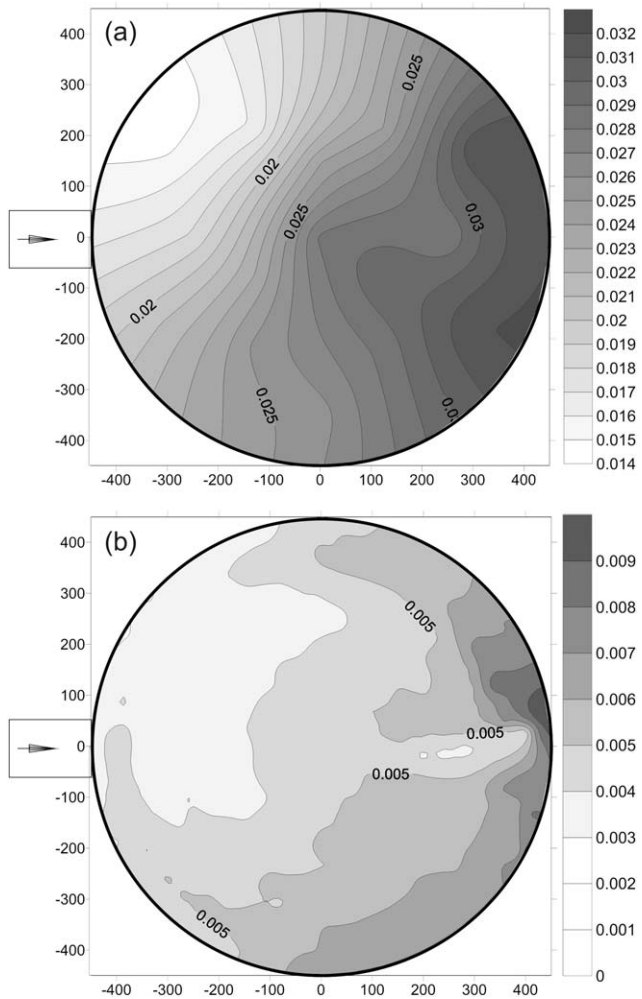

Figure 19. Distribution topograms for local concentration in column cross-section at the level of the sixth packing layer (a) and under the packing (b) at uniform liquid irrigation.

$L/V = 1.7$. $F_v = 1.34$ Pa$^{1/2}$; $w_L = 6.19 \times 10^{-3}$ m/s.

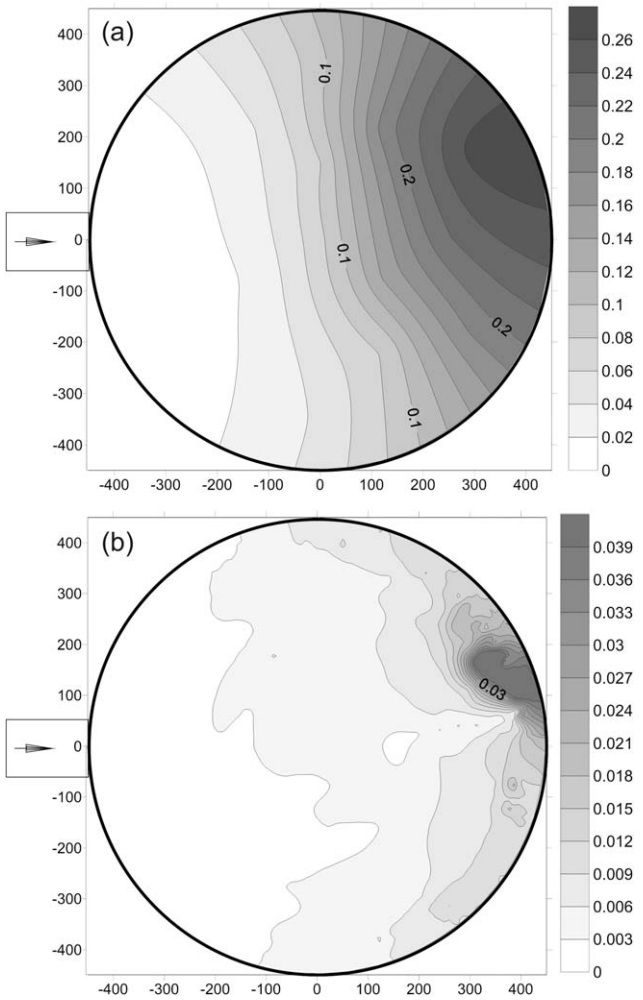

Figure 20. Distribution topograms of local concentration in the column cross-section at the level of the sixth packing layer (a) and under the packing (b) Rows No. 1, 2 are blocked.

$F_v = 1.25$ Pa$^{1/2}$, $w_L = 3.75 \times 10^{-3}$ m/s.

the symmetrical character with diametrically opposite maximum and minimum. The similar character of concentration distribution was obtained for other values of w_L and F_v. It should be only noted that with a rise in vapor velocity we can observe some systematic clockwise displacement of the pole with increased concentration near the wall. It follows from data analysis that temperature difference in the packing cross-section at the level of the sixth layer is 5–6 K in experiments with $L/V = 1$ and 0.6–0.7 K in experiments with $L/V = 1.7$. At that the temperature difference along the whole column is (7–8) K and (4–5) K, respectively. This considerable temperature maldistribution has been already shown in experiments with the aluminum 500Y packing in Pavlenko et al.,[10] and it can be connected with instability under the conditions of negative stratification of vapor density along the column height.

Distributions of concentration over the packing cross-section at the level of the sixth layer and distributions of liquid concentration over the column cross-section under the packing at $L/V = 1$ and different versions of hole blocking in the liquid distributor are compared in Figures 20–22. According to these figures, considerable temperature maldistribution over the packing cross-section at the level of the sixth layer as at uniform irrigation is also observed. This maldistribution has the similar symmetrical character with diametrically opposite maximum and minimum both at the level of the sixth layer and at the packing outlet. The degree of maldistribution on the sixth layer is higher in the case of nonuniform irrigation in comparison with uniform irrigation at the same operation parameters. The position of maximum and minimum stays the same at minimal liquid loads $w_L = 2.08 \times 10^{-3}$ m/s for uniform irrigation and for the case of two blocked rows. In other cases, we can observe counterclockwise poles displacement at nonuniform irrigation approximately by 30–60°. This means that the direction of maximal temperature gradient at nonuniform packing irrigation almost coincides with the direction of maximal gradient of initial nonuniformity in packing irrigation. Perhaps, considerable maldistribution of irrigation at the packing inlet causes formation of temperature maldistribution over the column cross-section, which spreads along the whole height of the packing without a change in orientation. It was found out that the location of zones with a higher temperature (and,

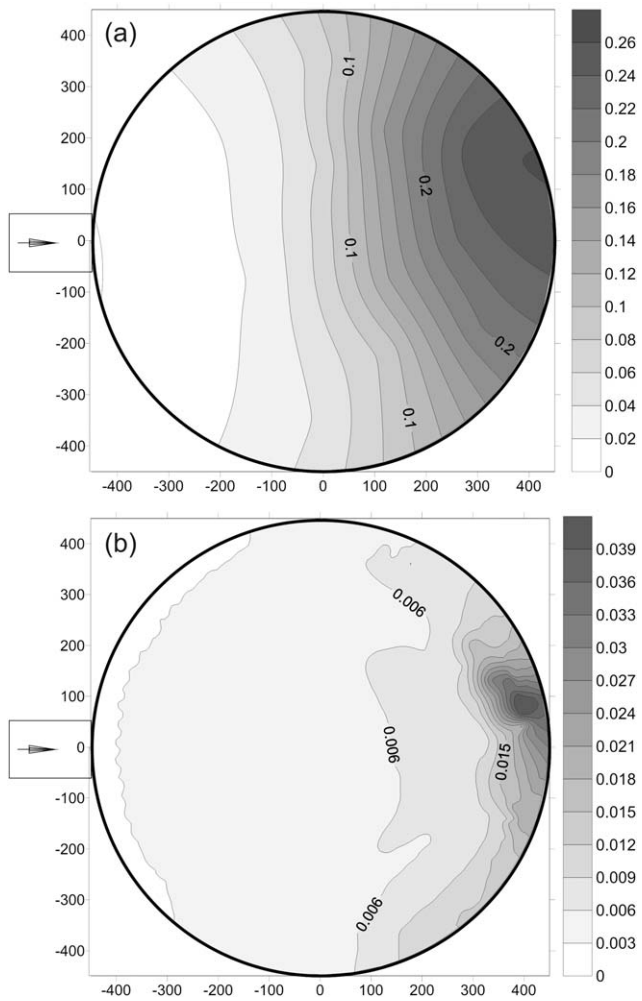

Figure 21. Distribution topograms of local concentration in the column cross-section at the level of the sixth packing layer (a) and under the packing (b) No. 1 is blocked.

$F_v = 1.25$ Pa$^{1/2}$; $w_L = 3.78 \times 10^{-3}$ m/s.

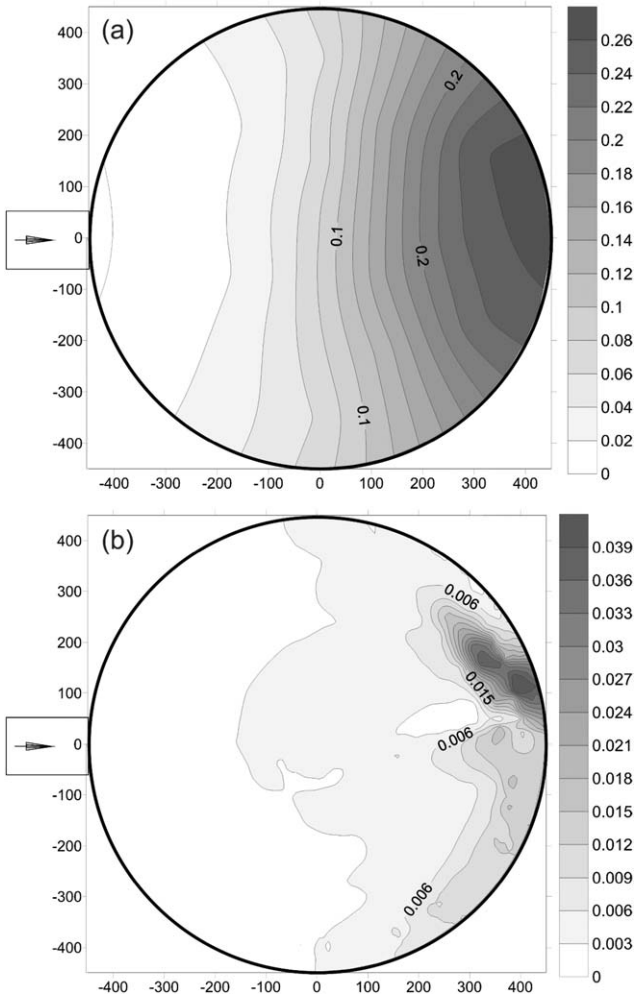

Figure 22. Distribution topograms of local concentration in the column cross-section at the level of the sixth packing layer (a) and under the packing (b) No. 2 is blocked.

$F_v = 1.27$ Pa$^{1/2}$; $w_L = 3.86 \times 10^{-3}$ m/s.

hence, with lower concentration) usually matches the position of zones with minimal density of packing irrigation in the current experimental series. It also follows from analysis of data that the positions of large-scale zones of maximal concentration over the column cross-section on the sixth packing layer and under the packing almost coincide for all operation parameters used in experiments (e.g., see Figures 18–22).

Analysis of experimental data obtained shows that efficiency of mixture separation on the 19-layer structured packing depends essentially on the value of L/V, vapor flow factor F_v, liquid load w_L, and size of the zone irrigated insufficiently by the liquid distributor. At that, according to measurements on distribution of local liquid flow rate over the column cross-section and wall, distributions of temperature and concentration of mixture over the column cross-section and along the height, the distribution character of the above parameters changes weak along the height in the lower part of the column at a change in maldistribution degree of irrigation by the liquid distributor. This indicates that the determined character of significantly nonuniform distribution of the above parameters of the liquid and vapor flows over the cross-section is formed and stabilized in the upper layers (parts) of the column.

Conclusions

I

1. At $L/V = 1$, in the range of small vapor flow rates separation efficiency on the Mellapak 350.Y packing decreases with a decrease in vapor load and, hence, the liquid load. At high F_v and w_L, when the packing surface is more wet, the HETP value stays almost constant. At $L/V = 1.7$ efficiency of mixture separation is almost constant in the whole range of parameter F_v. The HETP value at $L/V = 1.7$ decreases twice in comparison with corresponding values within the plateau at $L/V = 1$.
2. The effect of nonuniformity of packing irrigation on separation efficiency depends on the degree of maldistribution. Blocking of 10% of drip points in one half of column cross-section increases HETP by 10–12% independently on the value of L/V. Blocking of 20% of drip points deteriorates separation efficiency by 30–35% at $L/V = 1$ and by $\approx$50% at $L/V = 1.7$. The higher the number of theoretical plates of separation at uniform packing irrigation, the higher the relative effect of large-scale nonuniformity of irrigation on reduction of separation efficiency.
3. In the studied ranges of liquid and vapor flow rates, the relative pressure drop on the packing depends on parameter F_v and does not depend on the ratio of liquid and vapor flow rates L/V and degree of irrigation maldistribution at the inlet.
4. The zone of increased flow rate at the packing periphery (an excess of 20–25%) is typical for distribution of the local density of liquid flow rate over the column cross-section. At sufficiently high values of F_v, the zone with increased flow rate at the periphery is smoothed over. With a rise of w_L, we observe the formation of the zone with increased flow rate in the center of column cross-section.
5. Creation of nonuniform irrigation of the packing via the blocking of 10 and 20% of holes did not effect the distribution character of the liquid flow rate density at the outlet of 19-layer packing.
6. For all parameters w_L and F_v, we observe significant maldistribution of liquid temperature and concentration over the cross-section inside the packing. Maldistribution has the symmetrical character with diametrically located maximum and minimum. The temperature difference in cross-section is comparable with total temperature difference along the column height in experiments with $L/V = 1$ and it equals 15–20% of the total difference along the column height in experiments with $L/V = 1.7$. Distribution of liquid concentration under the packing is nonuniform over the cross-section. Diametrically opposite zones of minimal and maximal concentration are observed. The positions of zones with minimal and maximal concentration in cross-section of the sixth layer of the packing and in column cross-section under the packing almost coincide. At that the measured total efficiency of the packing at $L/V = 1$ corresponds to the expected one, that is, measured before by means of other systems (for instance, Fractionation Research, Inc. (FRI)).

7. Creation of nonuniformity in packing irrigation by blocking of 10 and 20% of distributor holes initiates formation of temperature maldistribution over the column cross-section, which spreads along the whole height of the packing without a change in its orientation. The position of zones of a higher temperature (and, hence, lower concentration) corresponds to position of zones with lower density of packing irrigation.
8. Analysis of temperature distribution thermograms over the packing cross-section shows that during transition to stable column operation the temperature and concentration of liquid at the initial period are almost uniform over the cross-section. When some degree of mixture separation is achieved, instability of the liquid and vapor counter flows in the packing develops, and a significant temperature and concentration gradient is formed in the column cross-section.

II

1. Efficiency of mixture separation can be improved by installation of intermediate redistributors of liquid and vapor, which eliminate the negative influence of local liquid flow rate and mixture concentration maldistributions in the packing cross-section and on the column wall. Design of intermediate redistributors of liquid and vapor should ensure the leveling of liquid and vapor flow rates over the column cross-section as well as the leveling of mixture concentration in liquid and vapor phases. To determine the optimal position of liquid and vapor redistributors along the column height and develop its efficient and practically feasible design, the following studies with a lesser number of layers are required.
2. The important conclusion of the current study is the fact that the use of liquid and vapor redistributors should be based on consideration of a number of parameters associated with the function of a change in the liquid and vapor maldistribution factor f_{max} along the column height, and total efficiency of mixture separation at the given height of the real packing. According to analysis of experimental data, even at relatively uniform distribution of liquid we can observe highly significant maldistribution of mixture temperature and concentration over the packing cross-section along its whole height. To answer the main question (what is the maximal height of a specific packing?/How often the redistributor should be used for this packing?), it is necessary to study in detail the local distribution of liquid and vapor with consideration the effect of poorly studied factor of negative vapor stratification by density, which is formed at real mixture separation in the structured packing. It is obvious that the necessity for installation of liquid and vapor redistributors is determined not only by the requirements for smoothing the vapor and liquid flow rates, but also smoothing the local temperatures and concentrations of liquid and vapor flows over the cross-section. Therefore, in terms of developing methods to control liquid and vapor flows in the packing and designing workable distributing systems, investigation of liquid and vapor counter flows hydrodynamics and its interconnection with separation efficiency using the liquid distributors with dynamically variable characteristics of packing cross-section irrigation seems to be very promising. In the same respect the use of irrigation systems, controlled by the given laws, and systems of vapor inlet/outlet in the certain zones of the packing cross-section in subsequent experiments with application of the modern control equipment, seems to be of a particular interest. The multipurpose experimental setup "Freon column" provides a possibility to study regularities of the counter flows of liquid and vapor in the structured packing under the of mixture separation conditions at different liquid irrigation modes and use of various liquid and vapor redistributors. The following comprehensive studies at this experimental setup on distributions of local characteristics (flow rate, temperature, mixture composition in the distillation process) of liquid and vapor flows and their interconnection with separation efficiency at different modes of liquid irrigation and vapor flows control with the use of various packing will be focused on testing the suggested approaches and ideas.

Acknowledgments

This work was supported by the Russian Academy of Sciences, project No. III.18.2.3 and by the BASF SE (Germany) and Air Products and Chemicals.

Notation

A = area of column cross-section, m^2
$C = (y_e - x)$ = concentration difference
dP = pressure drop, Pa
$F_v = U_v\sqrt{\rho_v}$ = vapor flow factor, $Pa^{1/2}$
HETP = height, equivalent to the theoretical plate, m
HTU = height of transfer unit, m
H = total height of the packing, m
L = molar flow rate of liquid, kmol/s
L/V = ratio of mole flow rates of liquid and vapor
p = pressure in the column, Pa
T = temperature, °C;
U = superficial velocity, m/s
V = molar flow rate of vapor, kmol/s
V_L = volumetric flow rate of liquid, m^3/s
$w_L = \frac{V_L}{A}$ = liquid load, $m^3/(m^2\ s)$
x = mole fraction of volatile component in the liquid phase
y = mole fraction of volatile component in the vapor phase
ρ = density, kg/m^3

Subscripts

ave = averaged
bot = column bottom
e = equilibrium
l = liquid
i = index
top = column top
v = vapor

Literature Cited

1. Leontiev VS, Sidorov SI. Modern packing columns: features of construction. *Khim Prom.* 2005;82:347–356.
2. Grunig J, Kim S-J, Kraume M. Liquid film flow on structured wires: fluid dynamics and gas-side mass transfer. *AIChE J.* 2013;59:295–302.
3. Hanley B, Chen C-C. New mass-transfer correlations for packed towers. *AIChE J.* 2012;58:132–152.
4. Pushnov AS. The effect of geometrical characteristics of the random metal packing of the blade type on hydraulic resistance and efficiency of heat and mass transfer in the column apparatuses. *Khim Prom.* 2012;89:222–229.
5. Olujic Z. Standardization of structured packing efficiency measurements. In: Handbook, Version 2. Delft, The Netherlands: Process and Energy Department, Delft University of Technology, 2010:1–65.
6. Pavlenko AN, Zhukov VE, Pecherkin NI, Chekhovich VY, Sunder S, Houghton P. Experimental study of the effect of maldistribution

at the structured packing inlet on the Freon mixture separation efficiency. *Theor Found Chem Eng*. 2009;43:1–11.
7. Alekseenko SV, Markovich DM, Evseev AR, Bobylev AV, Tarasov BV, Karsten VM. Experimental investigation of liquid distribution over structured packing. *AIChE J*. 2008;54:1424–1430.
8. Pavlenko AN, Pecherkin NI, Chekhovich VY, Volodin OA. Hydrodynamics in falling liquid films on surfaces with complex geometry. *Microgravity Sci Technol*. 2009;21:207–213.
9. Trifonov Y, Sunder S, Houghton P. Modeling of mixture separation in column with structured packing. Effect of liquid maldistribution. Distillation and Absorption 2006, IChemE Symposium Series 152, London, UK: Institution of Chemical Engineers, 2006:764–772.
10. Pavlenko AN, Zhukov VE, Pecherkin NI, Chekhovich VY, Sunder S, Houghton P. Development of non-uniformity in distribution of mixture composition in the structured packing of distillation column. *Theor Found Chem Eng*. 2010;44:869–876.
11. Mahr B, Mewes D. Modeling and measurement of macroscopic flow fields in structured packings. *Distillation and Absorption 2006, IChemE Symposium Series 152*, London, UK: Institution of Chemical Engineers, 2006:544–553.
12. Valluri P, Matar O, Mendes M, Hewitt G. Modelling hydrodynamics and mass transfer in structured packings-a review. *Multiphase Sci Technol*. 2002;14:303–348.
13. Taylor R. Distill modeling after all these years: a view of the state of the art. *Distillation and Absorption 2006, IChemE Symposium Series 152*, London, UK: Institution of Chemical Engineers, 2006:1–20.
14. Shilkin A, Kenig E. Separation performance of structured packed columns: a comparison of two modelling approaches. *Distillation and Absorption 2006, IChemE Symposium Series 152*, London, UK: Institution of Chemical Engineers, 2006:211–219.
15. Ataki A, Kolb P, Bühlman U, Bart H-J. Wetting performance and pressure drop of structure packings: CFD and experiment. *Distillation and Absorption 2006, IChemE Symposium Series 152*, London, UK: Institution of Chemical Engineers, 2006:534–543.
16. Boyer C, Fanget B. Measurement of liquid flow distribution in trickle bed reactor of large diameter with a new gamma-ray tomographic system. *Chem Eng Sci*. 2002;57:1079–1089.
17. Behrens M. Hydrodynamics and mass transfer performance of modular catalytic structure packing. PhD Thesis, The Netherlands: TU Delft, 2006.
18. Ottenbacher M, Olujić Ž, Jödecke M, Großmann C. Structured packing efficiency - vital information for the chemical industry. *Distillation and Absorption, 2010*, Eindhoven, The Netherlands: Eindhoven University of Technology, 2010:575–580.
19. Perry D, Nutter DE, Hale A. Liquid distribution for optimum packing performance. *Chem Eng Prog*. 1990;86:30–35.
20. Bonilla JA. Don't neglect liquid distributors. *Chem Eng Prog*. 1993; 89:47–61.
21. Gunn DJ, Al-Saffar HBS. Liquid distribution in packed columns. *Chem Eng Sci*. 1993;48:3845–3854.
22. Hoek P, Wesselingh J, Zuiderweg F. Small scale and large scale liquid maldistribution in packed columns. *Chem Eng Res Des*. 1986;64: 431–449.
23. Olujic Z, de Graauw J. Experimental studies on the interaction between the initial liquid distribution and the performance of structured packings. *Sep Sci Technol*. 1990;25:1723–1735.
24. Olujic Z, van Baak R, Haaring J. Liquid distribution behaviour of conventional and high capacity structured packings. *Distillation and Absorption 2006, IChemE Symposium Series 152*, London, UK: Institution of Engineers, 2006:252–266.
25. Pavlenko AN, Pecherkin NI, Chekhovich VY, Sunder S, Houghton P, Serov AF, Nazarov AD. Large industrial-scale model of structured packing distillation column. *J Eng Thermophys*. 2005;13:1–18.
26. Pavlenko AN, Pecherkin NI, Chekhovich VY, Sunder S, Houghton P, Serov AF, Nazarov AD. Distribution of a liquid on a structured packing in a large-scale model of a distillation column. *Theor Found Chem Eng*. 2006;40:329–338.
27. Marchot P, Toye D, Pelsser A-M, Crine M, L'Homme G, Olujic Z. Liquid distribution images on structure packing by X-ray computed tomography. *AIChE J*. 2001;47:1471–1476.
28. Shaibal R, Kemoun A, Al-Dahhan MH, Dudukovic MP, Skourlis TB, Dautzenberg FM. Countercurrent flow distribution in structure packing via computed tomography. *Chem Eng Process*. 2004;44:59–69.
29. Olujic Z, Mohammed Ali A, Jansens PJ. Effect of the initial gas maldistribution on the pressure drop of structure packing. *Distillation and Absorption 2002 Proceedings*, Baden-Baden, Germany: VDI, 2002:6–14.
30. Serov AF, Pavlenko AN, Pecherkin NI, Nazarov AD, Zhukov VE. Bubble flow meter for the study of the jet-droplet flow in the mass-transfer apparatuses. *Instrum Exp Tech*. 1998;5:145–149.
31. Lockett MJ, Billingham JF. The effect of maldistribution on separation in packed distillation columns, paper 2.2-2. *Distillation and Absorption 2002 Proceedings*, Baden-Baden, Germany; VDI, 2002.

Manuscript received July 2, 2013, and revision received Oct. 12, 2013.